International Journal of Fracture Fatigue and Wear, Volume 3

Proceedings of the 4th International Conference On
Fracture Fatigue and Wear, pp. 265-271, 2015

AN EFFICIENT COMPUTATIONAL APPROACH FOR NONLINEAR ANALYSIS OF SMART PIEZOELECTRIC PLATES

P. Phung-Van[1], Loc V. Tran[1], M. Abdel-Wahab[1], H. Nguyen-Xuan[2]

[1]Department of Mechanical Construction and Production, Faculty of Engineering and Architecture, Ghent University, Belgium
[2]Faculty of Mathematics & Computer Science, University of Science, Vietnam National University, Ho Chi Minh City, Vietnam

Abstract: In this paper, a simple and effective formulation based on isogeometric finite elements (IGA) for geometrically nonlinear analysis of FGM plates integrated with sensors and actuators is investigated. The nonlinear formulation is based on a generalized five-parameter displacement field of higher order shear deformation (HSDT) and the von Kármán strains, which includes thermo-piezoelectric effects. The electric potential of each piezoelectric layer is assumed linearly through the thickness of each piezoelectric layer. The material properties of FGM are assumed to vary through the thickness by the rule of mixture and the Mori–Tanaka scheme. The accuracy and reliability of the proposed method is verified by comparing its numerical solutions with those of available other numerical results.

Keywords: geometrically nonlinear, isogeometric analysis (IGA), functionally graded material plates (FGM), sensors and actuators.

1 INTRODUCTION

The integration of piezoelectric and FGM has many practical applications such as smart material systems, the medical, micro-electromechanical systems (MEMS) and aerospace industries [1], etc. Because of properties of thermo-electro-mechanical coupling, many methods have been proposed He et al. [2] developed a finite element model based on variational principle and linear piezoelectricity theory. The active control of FGM integrated with piezoelectric sensors and actuators was studied by Liew et al. [3]. The behaviour of a FGM piezoelectric plate in thermal environments using HSDT was investigated in Refs. [4,5]. Yang et al. [6] examined the nonlinear thermo-electro-mechanical bending response of piezoelectric FGM plates. The FE formulations based HSDT for nonlinear analysis of functionally graded piezoelectric plates were also reported in [7]. Recently, isogeometric analysis (IGA) of the piezoelectric composite plates using HSDT was studied by Ref. [8]. However, nonlinear transient analysis has not taken into account for their previous work. So far, there are few published materials related to geometrically nonlinear analysis using IGA for composite plates. Apparently, there are no study on nonlinear analysis based on isogeometric analysis using the generalized shear deformation theory for the piezoelectric FGM plates. So, this paper hence tries to fill this gap by using IGA based on the generalized shear deformation theory for geometrically nonlinear transient analysis of the piezoelectric FGM plates. The nonlinear formulation is based on a generalized higher order shear deformation (HSDT) and the von Kármán strains, which includes thermo-piezoelectric effects. The electric potential of each piezoelectric layer is assumed linearly through the thickness of each piezoelectric layer. The material properties of FGM are assumed to vary through the thickness by the rule of mixture and the Mori–Tanaka scheme. The accuracy and reliability of the proposed method is verified by comparing its numerical solutions with those of available other numerical results.

2 THE GENERALIZED HSDT FOR SMART PIEZOELECTRIC PLATES

2.1 The piezoelectric FGM model

A sandwich plate shown in Figure 1a has the volume fraction of ceramic and metal phase across thickness as follows

$$V_c(z)=\left(\frac{1}{2}+\frac{z_c}{h_c}\right)^n, \quad V_m(z)=1-V(z) \tag{1}$$

where *c* and *m* refer to the ceramic and metal, respectively; $z_c \in [z_2,\ z_3]$ and $h_c = z_3 - z_2$ is thickness of core which are displayed in Figure 1b. The material constituents of piezoelectric FGM can be obtained as:

$$V_c(z) = 1, \quad h_c \in [z_1,\ z_2];\ V_c(z) = \left(\frac{1}{2} + \frac{z_c}{h_c}\right)^n, \quad h_c \in [z_2,\ z_3] \text{ for core}$$
$$V_c(z) = 1, \quad h_c \in [z_3,\ z_4];\ V_m(z) = 1 - V_c(z) \tag{2}$$

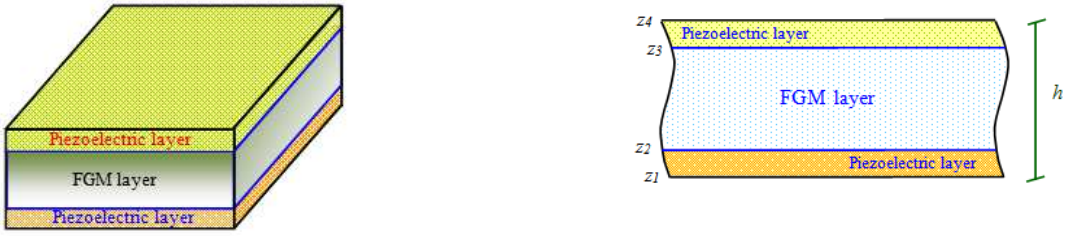

(a) (b)

Fig. 1 (a) Configuration of a piezoelectric FGM plate; (b) The sandwich plate with piezoelectric skins and FGM core

The material properties including Young's modulus (*E*), Poisson's ratio (*v*) and density (*ρ*) based on the mixture rule are defined by:

$$P = P_c V_c(z) + P_m V_m(z) \tag{3}$$

where P_c, P_m represent the individual properties of material of ceramic and metal. To consider the interactions among the constituents, the Mori-Tanaka scheme is used in this paper.

2.2 The generalized higher order shear deformation theory for piezoelectric FGM plates

In the piezoelectric FGM plates, there are two field variables including a mechanical displacements field and an electrical field that need to be approximated. The mechanical displacements are approximated by the generalized higher order shear deformation theory and expressed as follows

$$u = u_0 - z\partial w/\partial x + f(z)\beta_x;\ v = v_0 - z\partial w/\partial y + f(z)\beta_y;\ w = w \tag{4}$$

where u_0, v_0, β_x, β_y and *w* are displacement variables. The function *f*(*z*) is a continuous function through the plate thickness and chosen as $f(z) = h\arctan(2z/h) - z$ as in Thai *et al.* [9]

For a bending plate, the Green's strain vector can be presented by

$$\varepsilon_{ij} = \frac{1}{2}\left(\frac{\partial u_i}{\partial x_j} + \frac{\partial u_j}{\partial x_i}\right) + \frac{1}{2}\frac{\partial u_k}{\partial x_i}\frac{\partial u_k}{\partial x_j} \tag{5}$$

The material behaviour of piezoelectric FGM is expressed as following [10]

$$\begin{bmatrix} \boldsymbol{\sigma} \\ \mathbf{D} \end{bmatrix} = \begin{bmatrix} \mathbf{c} & -\mathbf{e}^T \\ \mathbf{e} & \mathbf{g} \end{bmatrix} \begin{bmatrix} \bar{\boldsymbol{\varepsilon}} \\ \mathbf{E} \end{bmatrix} \tag{6}$$

where $\boldsymbol{\sigma}$ and $\bar{\boldsymbol{\varepsilon}} = [\varepsilon\ \gamma]^T$ are the stress and strain vectors, respectively; **D** is the dielectric displacement; **e** is the piezoelectric constant matrix and **g** denotes the dielectric constant matrix; **E** is the electric field vector that is defined as

$$\mathbf{E} = -\text{grad}\phi \tag{7}$$

in which ϕ is the electric potential field; and **c** is the elasticity matrix and defined as

$$\mathbf{c}=\begin{bmatrix}\mathbf{A} & \mathbf{B} & \mathbf{N} & \mathbf{0}\\ \mathbf{B} & \mathbf{C} & \mathbf{F} & \mathbf{0}\\ \mathbf{N} & \mathbf{F} & \mathbf{H} & \mathbf{0}\\ \mathbf{0} & \mathbf{0} & \mathbf{0} & \mathbf{D}^{S}\end{bmatrix} \tag{8}$$

where

$$A_{ij},B_{ij},C_{ij},N_{ij},F_{ij},H_{ij}=\int_{-h/2}^{h/2}\left(1,z,z^2,f(z),zf(z),f^2(z)\right)\frac{E_e}{1-\nu_e^2}\begin{bmatrix}1 & \nu_e & 0\\ \nu_e & 1 & 0\\ 0 & 0 & \frac{1-\nu_e}{2}\end{bmatrix}\mathrm{d}z\ ,\quad i,j=1,2,6$$
$$D_{ij}^{S}=\int_{-h/2}^{h/2}\left[f'(z)\right]^2\frac{E_e}{2(1+\nu_e)}\begin{bmatrix}1 & 0\\ 0 & 1\end{bmatrix}\mathrm{d}z\ ,\qquad i,j=4,5 \tag{9}$$

And the piezoelectric constant matrix **e** and the dielectric constant matrix **g** are defined

$$\mathbf{e}=\begin{bmatrix}0 & 0 & 0 & 0 & d_{15} & 0\\ 0 & 0 & 0 & d_{15} & 0 & 0\\ d_{31} & d_{32} & d_{33} & 0 & 0 & 0\end{bmatrix}\ ;\quad \mathbf{g}=\begin{bmatrix}p_{11} & 0 & 0\\ 0 & p_{22} & 0\\ 0 & 0 & p_{33}\end{bmatrix} \tag{10}$$

3 THE SMART PIEZOELECTRIC PLATE FORMULATION BASED ON NURBS BASIC FUNCTION

Using Cox-de Boor algorithm, the univariate B-spline basis functions $N_{i,p}(\xi)$ are defined in Les Piegl and Wayne (1997) on the corresponding knot vector start with order p = 0

$$N_{i,0}(\xi)=\begin{cases}1 & \text{if}\quad \xi_i\le\xi<\xi_{i+1}\\ 0 & \text{otherwise}\end{cases} \tag{11}$$

as p + 1 the basis functions are obtained from

$$N_{i,p}(\xi)=\frac{\xi-\xi_i}{\xi_{i+p}-\xi_i}N_{i,p-1}(\xi)+\frac{\xi_{i+p+1}-\xi}{\xi_{i+p+1}-\xi_{i+1}}N_{i+1,p-1}(\xi) \tag{12}$$

To present exactly some conic sections, e.g., circles, cylinders, spheres, etc., non-uniform rational B-splines (NURBS) need to be used. Being different from B-spline, each control point of NURBS has an additional value called an individual weight $\zeta_A>0$.

$$R_A(\xi,\eta)=\frac{N_A(\xi,\eta)\zeta_A}{\sum_{A=1}^{m\times n}N_A(\xi,\eta)\zeta_A} \tag{13}$$

And the B-spline function is recovered as the individual weight of control point is constant.

3.1 Mechanical displacements

The displacement field **u** of the plate using NURBS basic function is approximated as

$$\mathbf{u}^h(\xi,\eta)=\sum_{I=1}^{m\times n}R_I(\xi,\eta)\mathbf{d}_I \tag{14}$$

where $\mathbf{d}_I=\left[u_{0I}\ v_{0I}\ \beta_{xI}\ \beta_{yI}\ w_I\right]^T$ is the vector of degrees of freedom associated with the control point I, and R_I is the shape function as defined in Eq. (13).

The strains can be expressed as

$$\bar{\boldsymbol{\varepsilon}}=[\boldsymbol{\varepsilon}\ \boldsymbol{\gamma}]^T=\sum_{I=1}^{m\times n}\left(\mathbf{B}_I^L+\frac{1}{2}\mathbf{B}_I^{NL}\right)\mathbf{d}_I \tag{15}$$

where $\mathbf{B}_I^L=\left[\left(\mathbf{B}_I^m\right)^T\ \left(\mathbf{B}_I^{b1}\right)^T\ \left(\mathbf{B}_I^{b2}\right)^T\ \left(\mathbf{B}_I^s\right)^T\right]^T$, in which

$$\mathbf{B}_I^m = \begin{bmatrix} R_{I,x} & 0 & 000 \\ 0 & R_{I,y} & 000 \\ R_{I,y} & R_{I,x} & 000 \end{bmatrix}, \mathbf{B}_I^{b1} = -\begin{bmatrix} 00 & R_{I,xx} & 00 \\ 00 & R_{I,yy} & 00 \\ 00 & 2R_{I,xy} & 00 \end{bmatrix}, \mathbf{B}_I^{b2} = \begin{bmatrix} 000 & R_{I,x} & 0 \\ 000 & 0 & R_{I,y} \\ 000 & R_{I,y} & R_{I,x} \end{bmatrix}, \mathbf{B}_I^s = \begin{bmatrix} 000 & R_I & 0 \\ 000 & 0 & R_I \end{bmatrix} \tag{16}$$

and $\mathbf{B}_I^{NL}$ is calculated by

$$\mathbf{B}_I^{NL}(\mathbf{d}) = \begin{bmatrix} w_{I,x} & 0 \\ 0 & w_{I,y} \\ w_{I,y} & w_{I,x} \end{bmatrix} \begin{bmatrix} 0 & 0 & R_{I,x} & 0 & 0 \\ 0 & 0 & R_{I,y} & 0 & 0 \end{bmatrix} = \mathbf{A}_\theta \mathbf{B}_I^g \tag{17}$$

3.2 Electric potential field

The electric potential field of each piezoelectric layer is approximated through the thickness as

$$\phi^i(z) = \mathbf{R}_\phi^i \boldsymbol{\phi}^i \tag{18}$$

where $\mathbf{R}_\phi^i$ is the shape functions for the electric potential which is defined in Eq. (13) with p = 1, and $\boldsymbol{\phi}^i$ is the vector containing the electric potentials at the top and bottom surfaces.

The electric field **E** in Eq. (7) can be rewritten as [10]

$$\mathbf{E} = -\nabla \mathbf{R}_\phi^i \boldsymbol{\phi}^i = -\mathbf{B}_\phi \boldsymbol{\phi}^i \tag{19}$$

3.3 Governing equations of smart piezoelectric plates

The governing equations for piezoelectric FGM plates can be written by

$$\underbrace{\begin{bmatrix} \mathbf{M}_{uu} & 0 \\ 0 & 0 \end{bmatrix}}_{\bar{\mathbf{M}}} \underbrace{\begin{bmatrix} \ddot{\mathbf{d}} \\ \ddot{\boldsymbol{\phi}} \end{bmatrix}}_{\ddot{\mathbf{q}}} + \underbrace{\begin{bmatrix} \mathbf{K}_{uu} & \mathbf{K}_{u\phi} \\ \mathbf{K}_{\phi u} & \mathbf{K}_{\phi\phi} \end{bmatrix}}_{\bar{\mathbf{K}}} \underbrace{\begin{bmatrix} \mathbf{d} \\ \boldsymbol{\phi} \end{bmatrix}}_{\mathbf{q}} = \underbrace{\begin{bmatrix} \mathbf{f} \\ \mathbf{q} \end{bmatrix}}_{\bar{\mathbf{f}}} \quad \Leftrightarrow \quad \bar{\mathbf{M}}\ddot{\mathbf{q}} + \bar{\mathbf{K}}\mathbf{q} = \bar{\mathbf{f}} \tag{20}$$

where

$$\begin{aligned} &\mathbf{K}_{uu} = \int_\Omega (\mathbf{B}^L + \mathbf{B}^{NL})^T \mathbf{c} (\mathbf{B}^L + \tfrac{1}{2}\mathbf{B}^{NL}) \mathrm{d}\Omega \quad ; \quad \mathbf{K}_{u\phi} = \int_\Omega (\mathbf{B}^L)^T \mathbf{e}^T \mathbf{B}_\phi \mathrm{d}\Omega \\ &\mathbf{K}_{\phi\phi} = \int_\Omega \mathbf{B}_\phi^T \mathbf{p} \mathbf{B}_\phi \mathrm{d}\Omega \quad ; \quad \mathbf{M}_{uu} = \int_\Omega \tilde{\mathbf{N}}^T \mathbf{m} \tilde{\mathbf{N}} \mathrm{d}\Omega \quad ; \quad \mathbf{f} = \int_\Omega \bar{q}_0 \bar{\mathbf{R}} \mathrm{d}\Omega \end{aligned} \tag{21}$$

in which $\bar{q}_0$ is a uniform load; $\bar{\mathbf{R}} = [0\,0\,0\,0\,R_I]$; **m** is defined by

$$\mathbf{m} = \begin{bmatrix} I_1 & I_2 & I_4 \\ I_2 & I_3 & I_5 \\ I_4 & I_5 & I_7 \end{bmatrix}, \quad (I_1, I_2, I_3, I_4, I_5, I_7) = \int_{-h/2}^{h/2} \rho \left(1, z, z^2, f(z), zf(z), f^2(z)\right) \mathrm{d}z \tag{22}$$

and

$$\tilde{\mathbf{N}} = \begin{Bmatrix} \tilde{\mathbf{N}}_1 \\ \tilde{\mathbf{N}}_2 \\ \tilde{\mathbf{N}}_3 \end{Bmatrix}, \tilde{\mathbf{N}}_1 = \begin{bmatrix} R_I & 0 & 0 & 0 & 0 \\ 0 & R_I & 0 & 0 & 0 \\ 0 & 0 & R_I & 0 & 0 \end{bmatrix}; \tilde{\mathbf{N}}_2 = -\begin{bmatrix} 0 & 0 & R_{I,x} & 0 & 0 \\ 0 & 0 & R_{I,y} & 0 & 0 \\ 0 & 0 & 0 & 0 & 0 \end{bmatrix}; \tilde{\mathbf{N}}_3 = \begin{bmatrix} 0 & 0 & 0 & R_I & 0 \\ 0 & 0 & 0 & 0 & R_I \\ 0 & 0 & 0 & 0 & 0 \end{bmatrix} \tag{23}$$

4 NUMERICAL EXAMPLES

4.1 Free vibration analysis

Consider a square Al2O3/Ti-6Al-4V plate (400mm × 400mm) with the thickness of the plate, *h*, is 5mm and thickness of each piezoelectric layer, *h_pie*, is 0.1mm. Figure 2 displays frequencies of the CCCC and SSSS plate. We can see that the frequencies of the present method match well with those of He et al. (2001) and those of the CCCC plate are larger than those of the SSSS plate.

4.2 Nonlinear analysis

4.2.1 An orthotropic plate

This example aims to verify the accuracy of the present method for geometrically nonlinear analysis. Consider a SSSS square plate subjected to a uniform loading of q_0 = 1 MPa. Material properties and the geometry are given E_1 = 525 GPa, E_2 = 21 GPa, $G_{12} = G_{23} = G_{13}$ = 10.5 GPa, v = 0.25, ρ = 800 kg/m^3, length L = 250 mm, thickness h = 5 mm. The normalized central deflection, $\bar{w} = w/h$, is shown in Figure 3. It can be observed that deflection responses of IGA match well with those of finite strip method (FSM) [11].

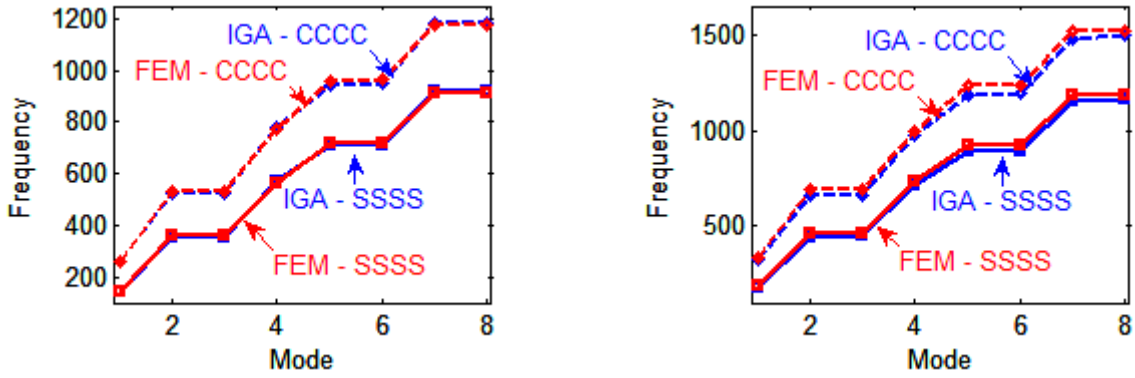

n = 0 n = 0.5

Fig. 2 The first lowest eight natural frequencies of the simply supported (SSSS) and clamped (CCCC) piezoelectric FGM plate with the different volume fraction exponents

4.2.2 A smart piezoelectric plate

Now we consider the square piezoelectric FGM plate with length L = 1, $h_{FGM} = L/20$ and $h_{piezo} = h_{FGM}/10$. The boundary condition of the plate is SSSS.

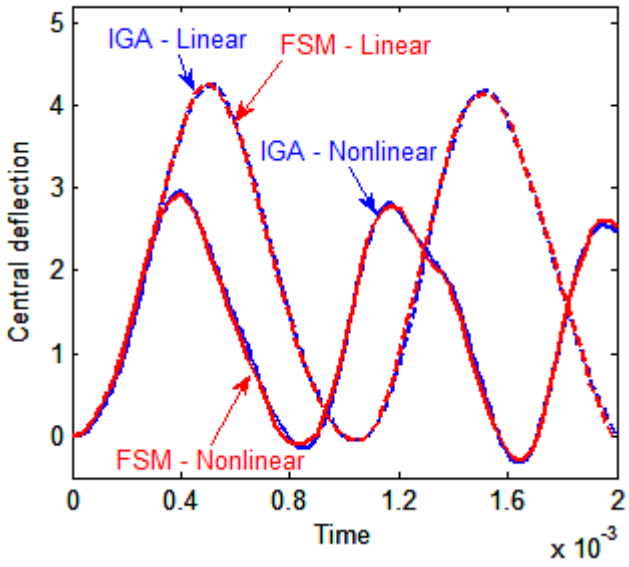

Fig. 3 Displacement of the plate under step uniform load

Figure 4a displays the effect of volume fraction exponent n to deflection of piezoelectric FGM (Al/ZrO2-2) plates under mechanical load (parameter load $\bar{q} = q_o \times 10^5$). It is seen that magnitude of deflection of nonlinear analysis is smaller than that of linear analysis. Next, effect of temperature to nonlinear deflection of the plate under thermo-mechanical load with n = 5 is displayed in Figure 4b. It is observed that the behaviour of deflection subjected to thermo-mechanical load is different from the pure mechanical loading. When the mechanical load is zero, the deflection of the plate is not zero. This is because of thermal expansion phenomenon. Also, the deflection decreases correspondingly to the increase of the temperature.

5 CONCLUSIONS

The paper presents a simple and effective formulation based on isogeometric finite elements (IGA) for geometrically nonlinear analysis of FGM piezoelectric plates. The nonlinear formulation is based on a generalized five-parameter displacement field of higher order shear deformation (HSDT) and the von Kármán strains, which includes thermo-piezoelectric effects. The electric potential of each piezoelectric layer is assumed linearly through the thickness of each piezoelectric layer. The material properties of FGM are assumed to vary through the thickness by the rule of mixture and the Mori–Tanaka scheme. The accuracy and reliability of the proposed method is verified by comparing its numerical solutions with those of available other numerical results.

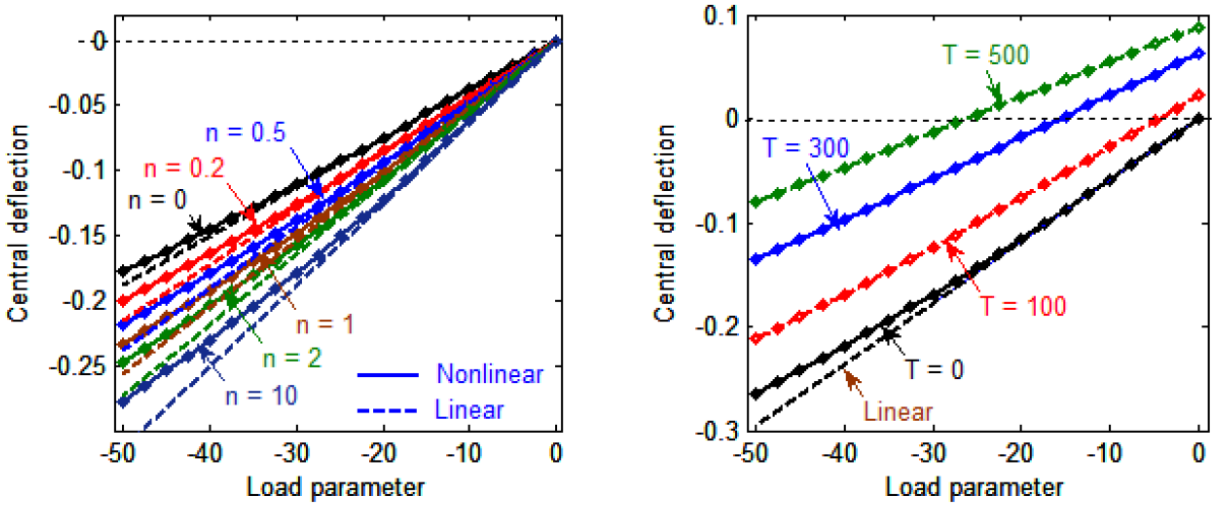

Fig.4 The first lowest eight natural frequencies of the simply supported (SSSS) and clamped (CCCC) piezoelectric FGM plate with the different volume fraction exponents

6 REFERENCES

[1] K. Takagi, JF. Li, S. Yokoyama, R. Watanabe, Fabrication and evaluation of PZT/Pt piezoelectric composites and functionally graded actuators, Journal of the European Ceramic Society, 23, 1577–1583, 2003

[2] XQ. He, TY. Ng, S. Sivashanker, KM. Liew, Active control of FGM plates with intergrated piezoelectric sensors and actuators, International Journal of Solids and Structures, 38, 1641-1655, 2001

[3] KM. Liew, XQ. He, TY. Ng, S. Kitipornchai, Finite element piezothermo-elasticity analysis and active control of FGM plates with integrated piezoelectric sensors and actuators, Computational Mechanics, 31, 350–358, 2003.

[4] P. Phung-Van, T Nguyen-Thoi, H Luong-Van, Q Lieu-Xuan, Geometrically nonlinear analysis of functionally graded plates using a cell-based smoothed three-node plate element (CS-MIN3) based on the C0-HSDT, Computer Methods in Applied Mechanics and Engineering, 270, 15-36, 2014.

[5] XL. Huang, HS. Shen, Vibration and dynamic response of functionally graded plates with piezoelectric actuators in thermal environments. Journal of Sound Vibration, 289, 25–53, 2006.

[6] J. Yang, S. Kitipornchai, KM. Liew, Non-linear analysis of thermo-electro-mechanical behaviour of shear deformable FGM plates with piezoelectric actuators. International Journal for Numerical Methods in Engineering, 59, 1605–1632, 2004.

[7] B. Behjat, MR. Khoshravan, Geometrically nonlinear static and free vibration analysis of functionally graded piezoelectric plates. Composites Structures, 94, 874–882, 2012.

[8] P. Phung-Van, L. De Lorenzis, Chien H. Thai, M. Abdel-Wahab, H. Nguyen-Xuan, Analysis of laminated composite plates integrated with piezoelectric sensors and actuators using higher-order shear deformation theory and isogeometric finite elements. Computational Materials Science, 96, 496-505, 2015.

[9] Chien H. Thai, AJM. Ferreira, SPA Bordas, T Rabczuk, H. Nguyen-Xuan, Isogeometric analysis of laminated composite and sanwich plates using a new inverse trigometic shear deformation theory, European Journal of Mechanics – A/Solids, 43, 89-108, 2014.

[10] P. Phung-Van, T. Nguyen-Thoi, T. Le-Dinh, H. Nguyen-Xuan, Static and free vibration analyses and dynamic control of composite plates integrated with piezoelectric sensors and actuators by the cell-based smoothed discrete shear gap method (CS-FEM-DSG3), Smart Materials and Structures, 22, 095026, 2013.

[11] J. Chen, DJ. Dawe, S. Wang, Nonlinear transient analysis of rectangular composite laminated plates, Composite Structures, 49, 129-139, 2000.